fermentation

MDPI

Article

β-Farnesene Production from Low-Cost Glucose in Lignocellulosic Hydrolysate by Engineered *Yarrowia lipolytica*

Haoran Bi, Chenchen Xv, Changsheng Su, Pan Feng, Changwei Zhang, Meng Wang *, Yunming Fang and Tianwei Tan *

National Energy Research Center for Biorefinery, Beijing University of Chemical Technology, Beijing 100029, China

* Correspondence: wangmeng@mail.buct.edu.cn (M.W.); biorefinery@mail.buct.edu.cn (T.T.)

Abstract: β-Farnesene is value-added acyclic volatile sesquiterpene with wide applications in energy, industry, and agriculture. Producing high-value-added compounds from low-cost renewable feedstocks in engineered microbial cell factories is an environmentally friendly and economical process for β-farnesene biosynthesis. In this study, the potential for using engineered *Yarrowia lipolytica* to produce β-farnesene from lignocellulosic hydrolysate as the carbon source was investigated. An efficient biosynthetic pathway for β-farnesene production was established via iterative enhancement of multiple genes based on the high endogenous acetyl-CoA flux in *Yarrowia lipolytica.* Overexpression of mevalonate pathway genes and screening of β-farnesene synthase resulted in a β-farnesene titer of 245 mg L^{-1} in glucose media. Additional copies of mevalonate pathway genes and enhanced expression of HMG-CoA reductase and β-farnesene synthase further increased the titer of β-farnesene to 470 mg L^{-1}. In addition, by combining metabolic engineering strategies using the lignocellulosic hydrolysate utilization strategy, the addition of Mg^{2+} promoted the production of β-farnesene, and the best-performing strain produced 7.38 ± 0.24 g L^{-1} β-farnesene from lignocellulosic hydrolysate media in a 2 L fermenter after 144 h. This study shows great potential for the sustainable production of β-farnesene from lignocellulosic biomass via engineered *Yarrowia lipolytica*.

Keywords: β-Farnesene; *Yarrowia lipolytica*; lignocellulosic hydrolysate; metabolic engineering; fed-batch fermentation

Citation: Bi, H.; Xv, C.; Su, C.; Feng, P.; Zhang, C.; Wang, M.; Fang, Y.; Tan, T. β-Farnesene Production from Low-Cost Glucose in Lignocellulosic Hydrolysate by Engineered *Yarrowia lipolytica*. *Fermentation* **2022**, *8*, 532. https://doi.org/10.3390/fermentation8100532

Academic Editors: Donatella Cimini and Luca Settanni

Received: 16 September 2022
Accepted: 5 October 2022
Published: 12 October 2022

1. Introduction

Farnesene is an acyclic volatile sesquiterpene that was first discovered in apple peel [1]. In nature, farnesene is mainly found in essential oils such as orange oil, rose oil, and tangerine oil, and it has two isoforms: α-farnesene and β-farnesene. As an aphid alarm pheromone, β-farnesene plays an important information transfer role in aphids. Therefore, β-farnesene was first applied as an agricultural protectant for pest control in agricultural production [2–4]. β-Farnesene has a suitable cetane number, fuel density, and low cloud point, which allows it to be used for the preparation of high-calorific-value, clean, renewable biofuels [5]. Vitamin E is one of the world's most common vitamin products, and the process of synthesizing vitamin E using β-farnesene as an intermediate can reduce carbon emissions by 60%, which is more environmentally friendly than the traditional chemical synthesis route. In addition, β-farnesene is also used in the production of lubricants, surfactants, and cosmetics [6]. Due to the extremely low content of β-farnesene in plants and the fact that plant growth is influenced by season and regional climate, the production of β-farnesene from plant extracts cannot meet the market demand. The yield of β-farnesene can reach 86% by chemical synthesis, but there are often isomers and by-products in chemically synthesized β-farnesene products, and the inevitable problems of high production cost, lack of availability of raw materials, and environmental pollution are still present [7,8].

With the recent development of metabolic engineering and synthetic biology, the production of β-farnesene using microbial cell factories has become an ideal alternative

to the traditional production route [9,10]. Previous studies have shown that several microorganisms serve as hosts for β-farnesene biosynthesis. For example, Yao et al. constructed mevalonate pathway-enhanced *Escherichia coli*, and the titer of β-farnesene reached 10.31 g L^{-1} when biodiesel byproducts were used as a substrate after fermentation optimization [11]. You et al. developed a recycling strategy for corncob pretreatment and cellulose hydrolysis, and recombinant *Escherichia coli* overexpressed with a heterologous ATP citrate lyase produced 4.06 g L^{-1} β-farnesene from corncob hydrolysate [12]. Several strategies have been applied with *Saccharomyces cerevisiae*, the most-used fungal host, to promote β-farnesene synthesis, such as deleting branching pathway genes, using affibody scaffold proteins for colocalization of farnesyl diphosphate synthase (ERG20) and BFS, and performing fed-batch cultivations with respiratory quotient (RQ) controlled feed [13–15]. By rewriting the central carbon metabolism of *Saccharomyces cerevisiae* with non-native reactions and carrying out multiple rounds of mutagenesis, a titer of 130 g L^{-1} of β-farnesene was produced from cane syrup, representing the highest level of production reported to date [16]. Shi et al. developed efficient β-farnesene production through overexpression of the mevalonate pathway and deletion of diacylglycerol o-acyltransferase 1 and diacylglycerol o-acyltransferase 2 (DGA1 and DGA2), and the recombinant *Yarrowia lipolytica* (*Y. lipolytica*) produced 22.8 g L^{-1} β-farnesene from glucose in fed-batch fermentation [17]. Although efficient production of β-farnesene has been achieved using sugar as a carbon source, the use of agricultural waste as a substrate has rarely been reported, especially in *Y. lipolytica*.

Y. lipolytica is a dimorphic yeast with sufficient intracellular acetyl-CoA supply and excellent ability to accumulate lipids. It can use a wide range of substrates for cell growth and product synthesis. In addition to the most common one, glucose, *Y. lipolytica* can also utilize unconventional carbon sources such as organic acids, polyols, and hydrophobic substrates [18,19]. Studies have reported using *Y. lipolytica* as a host for the biosynthesis of terpenoids such as β-farnesene, squalene, and β-carotene [17,20,21]. In *Y. lipolytica*, acetyl-CoA is converted to farnesyl pyrophosphate (FPP) via the mevalonate (MVA) pathway, and FPP is further catalyzed by BFS to generate β-farnesene; this process is accompanied by the consumption of ATP and NAD(P)H. Hydroxymethylglutaryl-CoA (HMG-CoA) reductase (HMGR) is the rate-limiting enzyme in the MVA pathway; it reduces HMG-CoA to mevalonate, an irreversible catalytic reaction that consumes two molecules of NADPH or NADH (Figure 1) [22]. Terpene production in microorganisms can be effectively promoted by enhancing the expression of mevalonate pathway enzymes and terpene synthases [23].

More environmentally friendly and sustainable technological and economic processes need to be developed due to the environmental crisis and population explosion. Converting lignocellulose into biofuels or advanced chemicals is very attractive because lignocellulose is a renewable, abundant, and cheap biomass on the planet [24]. Corn stover, one of the main types of agricultural waste, consists mainly of cellulose, hemicellulose, and lignin, of which the cellulose content is 39% [25]. China produces more than 300 million tons of corn stover each year, which can be returned directly to the field or used for pellet compression, feed addition, biomass energy production, etc. [26,27]. The burning of large amounts of straw can lead to high pollution loads and have a serious impact on the soil [28,29], and the comprehensive utilization rate of corn stover is less than 40% [26]. Glucose and xylose are the major components of lignocellulose and the main fermentable constituents of the hydrolysate [30,31]. The process of corn stover hydrolysate bioconversion has been established for ethanol, butanol, xylitol, and biohydrogen [32–35]. In this study, corn stover lignocellulosic hydrolysate was used as a carbon source for high-value-added β-farnesene production with *Y. lipolytica*.

The aim of this work was to investigate the ability to produce β-farnesene from lignocellulosic hydrolysate in engineered *Y. lipolytica*. Screening of β-farnesene synthase and two rounds of enhanced expression of the entire mevalonate pathway enhanced the metabolic flux of β-farnesene synthesis from glucose, and overexpression of NADH-dependent HMG-CoA reductase further improved the utilization of reduced power and

increased the β-farnesene titers. The lignocellulose hydrolysate concentration and metal ion species in the media were optimized in shake flasks to improve fermentation. Using the lignocellulosic hydrolysate media in a 2 L fermenter, efficient synthesis of β-farnesene from lignocellulosic hydrolysate was achieved.

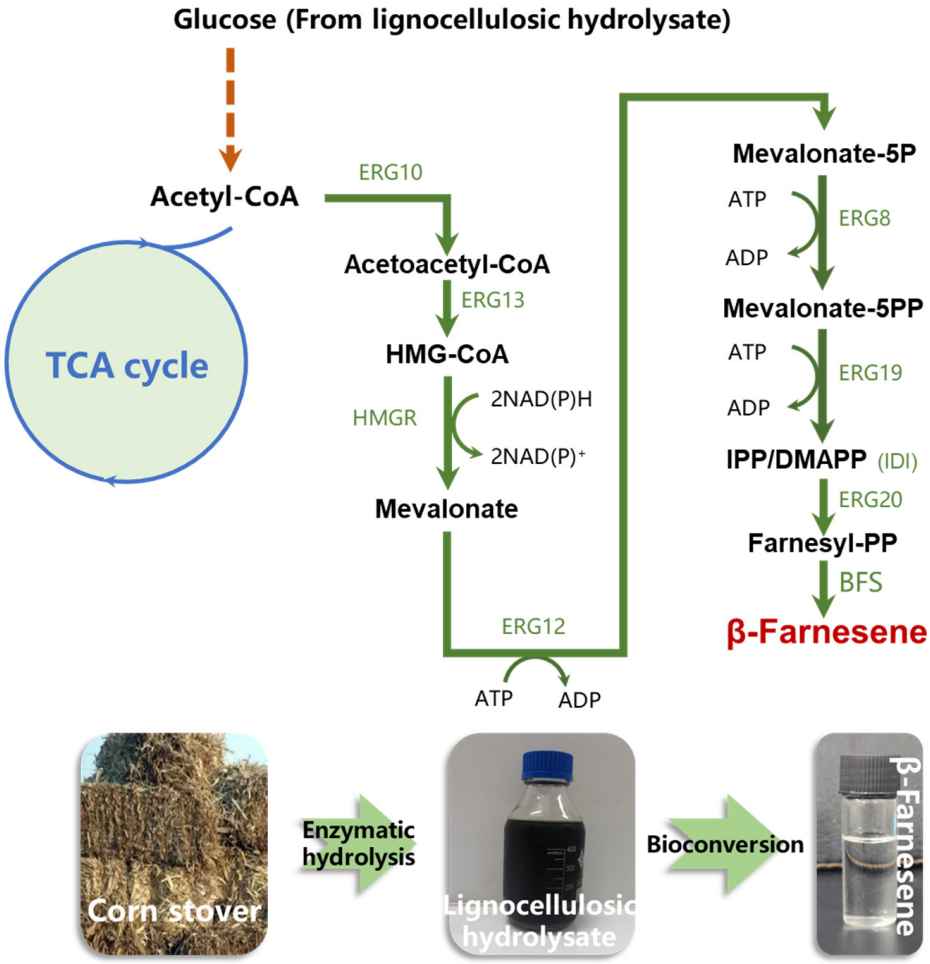

Figure 1. Production of β-farnesene from glucose in lignocellulosic hydrolysate and β-farnesene biosynthesis pathway in engineered *Y. lipolytica*. Pathway genes are shown in green, and dashed lines represent multi-step reactions. ERG10—acetoacetyl-CoA thiolase; ERG13—hydroxymethylglutaryl-CoA synthase; HMGR—hydroxymethylglutaryl-CoA reductase; ERG12—mevalonate kinase; ERG8—phosphomevalonate kinase; ERG19—mevalonate diphosphate decarboxylase; IDI—isopentenyl diphosphate isomerase; ERG20—farnesyl diphosphate synthase; BFS—β-farnesene synthase; IPP—isopentenyl diphosphate; DMAPP—dimethylallyl diphosphate; TCA—tricarboxylic acid.

2. Materials and Methods

2.1. Strains and Plasmid Construction

The plasmids used and constructed in this study are shown in Table S1. All plasmids were constructed by Gibson assembly [36]. The plasmid pRSFDuet1-HUH was used as a template to amplify the expression plasmid backbone and *Ura3* selection marker (hisG-*Ura3*-hisG sequence, HUH), and the endogenous genes, promoters, terminators, and homologous arm were cloned from the genome of *Y. lipolytica*. The primers used in this study are shown in Table S2. Primers and exogenous DNA were synthesized by BGI (Beijing, China). PrimeSTAR Max DNA polymerase (Takara Bio, Beijing, China) was used for amplification of DNA fragments. The exogenous DNA sequence is listed in Table S3. Specifically, endogenous genes *ERG10* (GeneID: 2907383), *ERG13* (GeneID: 2907642), *HMGR* (GeneID: 2912214), *ERG12* (GeneID: 2906793), *ERG8* (GeneID: 2912386), *ERG19*

(GeneID: 2907970), *IDI* (GeneID: 2907710), and *ERG20* (GeneID: 2911219), with their natural terminators, were linked to strong constitutive promoters his-ura-his box, homology arms, and plasmid pRSFDuet-HUH backbone via Gibson assembly for integration plasmid construction. For exogenous *nadh-HMGR*(AAV97299), *aaBFS* (AAX39387.1), *cjBFS* (AF374462.1), and *mcBFS* (KM586847.1), strong constitutive promoters and *XPR2* terminator were used for expression cassettes and integration plasmid construction. Repeated promoters, genes, or terminators were concatenated inversely to avoid fragment loss and ensure the stability of recombinant strains. All integration plasmids were linearized with primers for *Y. lipolytica* transformation (Table S1) and inserted into the specific sites of the *Y. lipolytica* chromosome based on a previous report [37].

The *Y. lipolytica* strain ATCC MYA2613 served as the host strain. *E. coli* Trans10 chemically competent cells (TransGen Biotech, Beijing, China) were used for plasmid construction, storage, and isolation. For the transformation of *Y. lipolytica*, competent cells were prepared by using a ZYMO Frozen-EZ Yeast Transformation II Kit (Zymo Research, Irvine, CA, USA). The linearized donor was concentrated with a vacuum concentrator, and 2–5 μg DNA was used for *Y. lipolytica* transformation. By harvesting transformants on a yeast nitrogen base without amino acids and ammonium sulfate (YNB)–Ura$^-$ solid medium (1.7 g L^{-1} YNB, 1 g L^{-1} amino acid mixture without uracil, 5 g L^{-1} ammonium sulfate, 20 g L^{-1} glucose, and 20 g L^{-1} agar powder) at 30 °C for 2 days, positive colonies were screened and checked by colony polymerase chain reaction (PCR). The selection marker was recovered by spreading cells on YPD–5-fluoroorotic acid (5-FOA) plates (10 g L^{-1} yeast extract, 20 g L^{-1} peptone, 20 g L^{-1} glucose, 20 g L^{-1} agar powder, and 1 μg L^{-1} 5-FOA). Strains used in this study are listed in Table 1.

Table 1. Strains used in this work.

Strain	Characteristics	Source
MYA2613	*matA, Ura3-302, Leu2-270, XPR2-322, Axp2-delta NU49,XPR2::SUC2*	ATCC
FY01	MYA2613 Δ*ku70*, Δ*ku80*:: *Leu2*	Lab storage
FY02	FY01 intA1:: *aaBFS*	This work
FY03	FY02 intC1:: *ERG10, tHMGR*, intC2:: *ERG12, ERG13*, intC3:: *IDI, ERG20*, intE1:: *ERG8, ERG19*	This work
FY04	FY03 Δ*aaBFS:: cjBFS*	This work
FY05	FY03 Δ*aaBFS:: mcBFS*	This work
FY06	FY03 intE2:: *ERG10, tHMGR*	This work
FY07	FY03 intE3:: *ERG12, ERG13*	This work
FY08	FY03 intE4:: *IDI, ERG20*	This work
FY09	FY03 intF1:: *ERG8, ERG19*	This work
FY10	FY09 intF2:: *tHMGR, tHMGR*	This work
FY11	FY09 intF2:: *nadh-HMGR, nadh-HMGR*	This work
FY12	FY09 intF2:: *nadh-HMGR, tHMGR*	This work
FY13	FY12 intF2:: *aaBFS*	This work
FY14	FY12 intF2:: *aaBFS, aaBFS*	This work

2.2. Fermentation Conditions

The fermentation performance of recombinant strains was tested in YNBG media (1.7 g L^{-1} YNB, 5 g L^{-1} ammonium sulfate, 40 g L^{-1} glucose, pH 6.0). Briefly, single colonies were scribed and activated on YPD plates and inoculated 2 days later in tubes containing 4 mL of YPD media, and then inoculated in 100 mL shake flasks containing 30 mL of YPD media. When cells grew to logarithmic growth phase, the culture was inoculated in 100 mL shake flasks containing 30 mL of YNBG media with an initial OD_{600} of 0.1 and cultured at 200 rpm and 30 °C for 96 h. After 60 h, 10% (v/v) n-nonane was added to collect β-farnesene. For the fermentation of lignocellulosic hydrolysate, YNBG media was replaced with lignocellulosic hydrolysate media (pH 6.0).

2.3. Pretreatment and Enzymatic Hydrolysis

The steam-exploded corn stover was obtained from COFCO Biochemistry Energy (Zhaodong) Co., Ltd. Following a previously described steam-explosion pretreatment protocol [38], the corn stover was composed of 44.2% glucan, 12.7% xylan, and 30.1% lignin. Cellic® CTec2, a commercial enzyme blend containing aggressive cellulases, a high level of β-glucosidase, and hemicellulose (Novozymes, Beijing, China), was used for enzymatic hydrolysis, and the cellulase loading rate was 20 FPU/g. Hydrolysis was performed at 50 °C and 180 rpm for 72 h in a 5 L reactor with a working volume of 3 L and a solid concentration of 10% (*w*/*v*), and the pH was adjusted to 4.8 with KOH. The hydrolysate was concentrated 2.5-fold with a rotatory vacuum evaporator at 65 °C and was then detoxified by activated carbon columns to remove inhibitors for fed-batch fermentation. The concentrated hydrolysate was passed through a glass column (10 mm in diameter, 200 mm in length) loaded with active charcoal (ratio of active charcoal mass to hydrolysate volume was 1:30) to remove inhibitors and obtain detoxified hydrolysate.

2.4. Fed-Batch Fermentation

The fed-batch fermentation was performed in a 2 L fermenter (xCUBIO twin, bbi-biotech) containing 500 mL of the initial 100% lignocellulosic hydrolysate media (40.3 ± 0.4 g L^{-1} glucose, 14.7 ± 0.3 g L^{-1} xylose, and 5 mM magnesium sulfate, pH 6.0). The activation process of the strain in fed-batch fermentation was similar to that in shake flasks, and the initial inoculum had an OD_{600} of 0.3. The fermentation temperature was set at 30 °C and the pH was kept at 6.0 using 3 M KOH. The initial stirring speed was set at 200 rpm and the aeration rate was set at 1 air volume/culture volume/min (1 vvm). For β-farnesene production, dissolved oxygen (DO) was maintained at 30 ± 5% by automatically controlling the stirring speed from 200 to 700 rpm. When the glucose in the fermentation broth was about to be depleted, the concentrated and detoxicated lignocellulose hydrolysate media (102.3 ± 0.6 g L^{-1} glucose, 37.6 ± 0.3 g L^{-1} xylose, and 5 mM magnesium sulfate, pH 6.0) was added to continue cell growth and β-farnesene production, and the fermentation process continued for 144 h. Subsequently, 10% (*v*/*v*) polyalphaolefin (PAO) was added to collect β-farnesene in the fermenter.

2.5. Analytical Methods

The optical density at 600 nm (OD_{600}) of appropriate diluted cultivation samples was determined using a spectrophotometer (Thermo Scientific, Waltham, MA, USA).

For the analysis of glucose, xylose, acetic acid, and citrate, cultivation samples and hydrolysis samples were centrifuged at 12,000 rpm for 3 min and then filtered with 0.22 μm films. Samples were detected by UltiMate 3000 HPLC (Thermo Scientific, Waltham, MA, USA) equipped with an RID detector and Bio-Rad Aminex HPX-87H column (Bio-Rad Laboratories, Hercules, CA, USA). The mobile phase was 5 mM H_2SO_4 and the flow rate was 0.6 mL min^{-1}, and the column and detector temperature was set at 65 °C.

Furfural and pentahydroxymethylfurfural were detected using an HPLC system with a C18 column (Waters Sunfire, 3.5 μm, 4.6 × 150 mm) and a 280 nm UV detector. The mobile phase was 70% (*v*/*v*) methanol/water with a flow rate of 1.0 mL min^{-1} and a column temperature of 30 °C. The soluble lignin content was measured with a spectrophotometer at a wavelength of 280 nm.

Coenzyme I NAD(H) Content Kit and Coenzyme II NADP(H) Content Kit (Suzhou Comin Biotechnology, Suzhou, China) were used to extract intracellular NADPH/$NADP^+$ and NADH/NAD^+, and a spectrophotometer (Thermo Scientific, Waltham, MA, USA) was used for detection.

For analysis of β-farnesene, the fermentation broth was centrifuged at 12,000 rpm for 5 min to collect the n-nonane or PAO layer and then diluted with ethyl acetate containing n-tetradecane internal standard. The mixed organic phase was analyzed by gas chromatography–mass spectrometry (GC-MS; 7890B GC/5977A MSD system, Agilent Technologies Inc., San Jose, CA, USA) equipped with an HP-5MS column (30 m × 250 μm × 0.1 μm; Agilent, USA).

The injection volume was 1 µL in split mode (1:20) and the injector temperature was 250 °C. Using 1.2 mL min^{-1} helium as the carrier gas, the oven program was set to 100 °C for 1 min, then raised by 10 °C min^{-1} to 240 °C and held for 1 min, and then ramped to 300 °C at 30 °C min^{-1} and held for 5 min.

2.6. Statistics

All data are given as mean ± standard deviation from 3 independent biological replicates (n = 3). Statistical analysis was performed with a 2-tailed *t*-test.

3. Results and Discussion

3.1. Construction of β-Farnesene Biosynthesis Pathway in Yarrowia lipolytica

Previous reports indicated that deleting endogenous DNA-binding proteins KU70 and KU80 in *Y. lipolytica* significantly reduced nonhomologous end-joining (NHEJ) efficiency and increased homologous recombination (HR) efficiency [20,39]. In this study, the *ku70* and *ku80* loci of *Y. lipolytica* MYA2613 were first knocked out and the leucine deficiency was restored (chromosomal integration of *Leu2* gene) to stabilize the fermentation phenotype, resulting in strain FY01.

β-Farnesene synthase gene from *Artemisia annua* (*Y. lipolytica* optimized codon, *aaBFS*) was integrated into strain FY01 under the control of strong constitutive P_{TEFin} promoter, resulting in strain FY02 [16,40]. The resulting strain produced 30 ± 5.6 mg L^{-1} of β-farnesene in YNBG shake flask media (Figure 2a). To direct cytoplasmic acetyl-CoA to the MVA pathway, we started with stepwise enhancement of endogenous *ERG10*, *ERG13*, *HMGR*, *ERG12*, *ERG8*, *ERG19*, *IdI*, and *ERG20* genes. These genes were inserted into strain FY02 chromosome under the control of strong constitutive P_{TEFin} promoter or P_{EXP1} promoter [41], resulting in strain FY03. Among them, *HMGR* acts as the rate-limiting enzyme of the MVA pathway to reduce hydroxymethylglutaryl-CoA to mevalonate. It has been shown that cleavage of the N-terminal sequence of the *HMGR* gene can avoid self-degradation of its N-terminal structural domain and improve the stability of its expression in the cytoplasm [20]. The sequence encoding the first 500 amino acids of the N-terminal of endogenous *HMGR* gene was deleted when amplified to obtain truncated *HMGR* (t*HMGR*). The titer of β-farnesene in strain FY03 increased by 7.2-fold (245 ± 16.3 mg L^{-1}) compared to that in strain FY02 (Figure 2a). As expected, overexpression of MVA pathway genes significantly enhanced the conversion of cytoplasmic acetyl-CoA to β-farnesene.

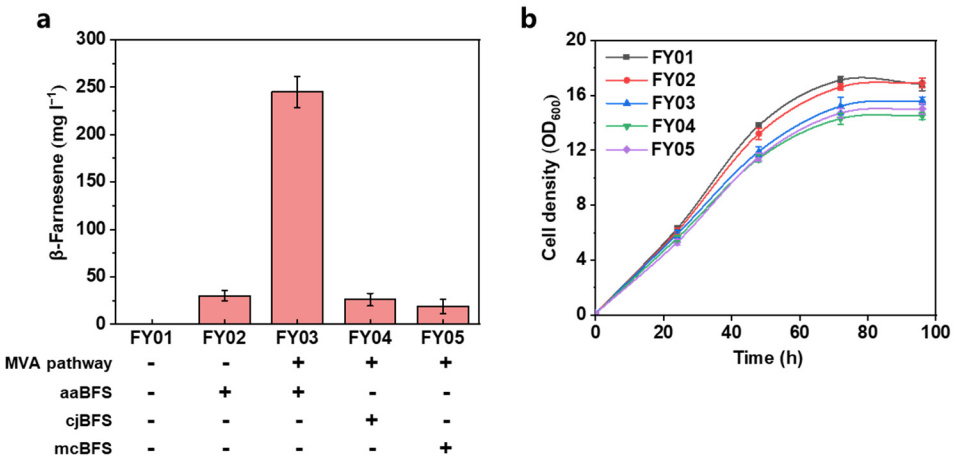

Figure 2. Construction of β-farnesene synthesis strain by overexpression of MVA pathway and β-farnesene synthase. Effect of expression of MVA pathway genes *aaBFS*, *cjBFS*, and *mcBFS* in strain FY01 on (**a**) β-farnesene production and (**b**) cell density. β-Farnesene was detected at 96 h of fermentation. Data are represented as mean ± standard deviation (n = 3).

We also tested two other β-farnesene synthases, from *Citrus junos* (*cjBFS*) and *Matricaria chamomilla var. recutita* (*mcBFS*). *CjBFS* and *mcBFS* were integrated into the chromosome of strain FY03 to replace *aaBFS* [2,42], resulting in strains FY04 and FY05, respectively. Obviously, the β-farnesene conversion efficiency of *cjBFS* and *mcBFS* (26 ± 6.6 mg L^{-1} and 19 ± 7.4 mg L^{-1}, respectively) in *Y. lipolytica* was much lower than that of *aaBFS* derived from *Artemisia annua* (Figure 2a). Therefore, we continued to use *aaBFS* as the β-farnesene synthase in the subsequent experiments of this study. Notably, the cell density of the strain with the enhanced endogenous MVA pathway was slightly lower than that of the initial strain (Figure 2b). This could be attributed to competition for cell growth due to upregulation of the MVA pathway or excessive accumulation of FPP due to low BFS enzyme activity [43,44].

3.2. Further Increasing the Carbon Flux of the MVA Pathway

The "push–pull" strategy has become a common approach in metabolic engineering to increase the metabolic flux of targeted synthetic pathways and improve target compound titers [40,45]. Considering that there may still have been excess cytosolic acetyl-CoA in the current strain, we performed additional overexpression of eight genes in the mevalonate pathway. Specifically, the eight genes were divided into four groups and integrated iteratively into strain FY03 under the control of strong constitutive P_{TEFin} promoter or P_{EXP1} promoter (*ERG10+tHMGR*, *ERG12+ERG13*, *IDI+ERG20*, *ERG8+ERG19*), resulting in strains FY06–FY09, respectively. It has been verified that *ERG10*, *HMGR*, *IDI*, and *ERG20* are particularly important for terpene synthesis among all MVA pathway genes [11,46,47]. Thus, these four genes were divided into two groups and were controlled using the TEFin promoter, which is the strongest natural constitutive promoter in *Y. lipolytica* [40]. ERG12, ERG13, ERG8, and ERG19 were divided into another two groups under the control of strong constitutive EXP1 promoter. As shown in Figure 3a, production of β-farnesene gradually increased with the integration of additional MVA pathway genes. Specifically, additional overexpression of *ERG10* and *tHMGR* in FY06 resulted in a β-farnesene titer of 315 ± 28.6 mg L^{-1}, which was 23% higher than that of FY05. The ERG10 gene encodes acetylacetyl-CoA thiolase, which is the first step in the MVA pathway, and pulls cytoplasm acetyl-CoA into the β-farnesene synthesis pathway. Elevated expression levels of *ERG10* and *tHMGR* have significant effects on β-farnesene synthesis. FY07 (additional *ERG12* and *ERG13*) produced a β-farnesene titer of 335 ± 31.3 mg L^{-1}, representing a 6.3% increase compared to FY06. Additional overexpression of *ERG12* and *ERG12* led to only a 3.4% increase in β-farnesene in FY08 (346 ± 17.9 mg L^{-1}) compared to FY07, while the β-farnesene titer of FY09 (additional *ERG8* and *ERG19*; 377 ± 29.7 mg L^{-1}) was further increased by 5.9% compared to FY08 (Figure 3a).

As we supposed, the enhanced MVA pathway flux made fuller use of cytoplasmic acetyl-CoA in *Y. lipolytica*. After further upregulation of eight MVA pathway genes, the β-farnesene production of FY09 was 47.3% higher than that of FY03, the control strain, and did not show further cytotoxicity (Figure 3b).

Endogenous *tHMGR* in *Y. lipolytica* catalyzes the NADPH-dependent reduction of hydroxymethylglutaryl-CoA. We considered that strain FY09 may still improve the MVA pathway flux through further overexpression of *HMGR*, but other than that, the intracellular NADH pool (mainly generated by the TCA cycle) was not used for β-farnesene synthesis. We tested *Silicibacter pomeroyi*-derived NADH-dependent *HMGR* (*nadh-HMGR*) to broaden the co-factor spectrum of HMG-CoA reduction [16]. Here, two copies of *tHMGR*, two copies of *nadh-HMGR*, and one copy each of *tHMGR* and *nadh-HMGR* were integrated into strain FY09 to obtain strains FY10, FY11, and FY12, respectively.

Compared with strain FY09, additional expression of two copies of *tHMGR* led to a 6.8% increase in β-farnesene titer in strain FY10 (395 ± 29.6 mg L^{-1}), while additional expression of two copies of *nadh-HMGR* further increased β-farnesene production by 14.9% in strain FY11 (425 ± 21.5 mg L^{-1}). FY12 showed the best improvement in β-farnesene titer among the three *HMGR*-enhanced strains (18.7% increase), with overexpression of one copy

each of *tHMGR* and *nadh-HMGR*, resulting in a final β-farnesene titer of 439 ± 29.3 mg L^{-1} (Figure 4a). The results indicate that overexpression of NADH-dependent *nadh-HMGR* played a positive role in further enhancing β-farnesene synthesis. There was no significant difference in growth status among the experimental strains, suggesting that the expression of high-copy number NAD(P)H-dependent HMG-CoA reductase did not cause a cellular metabolic burden (Figure 4b). According to the copy composition of HMG-CoA reductase in FY12, the optimal strain, the combination of three copies of *tHMGR* and one copy of *nadh-HMGR* was found to be the most beneficial to make full use of intracellular precursors and co-factors for β-farnesene synthesis.

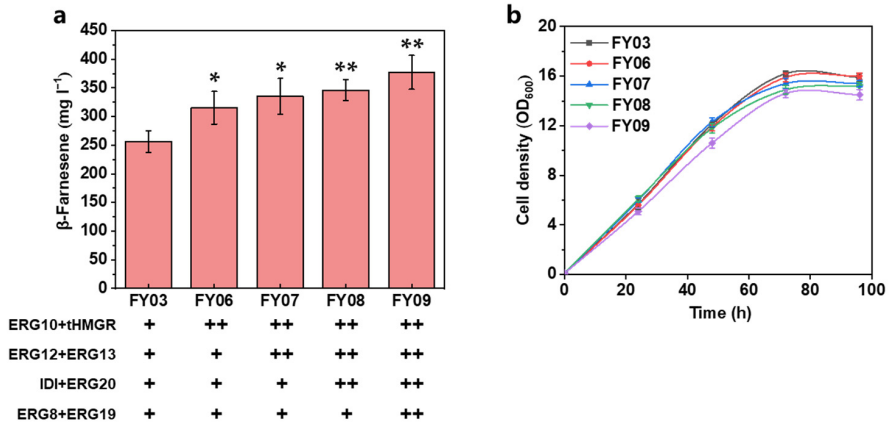

Figure 3. Second-round overexpression of eight genes in MVA pathway. (**a**) β-Farnesene production by iterative reinforcement of MVA pathway genes and (**b**) cell density. Each black plus sign represents a copy. β-Farnesene was detected at 96 h of fermentation. Data are represented as mean ± standard deviation (n = 3). Statistically significant differences between each engineered β-farnesene production strain and control strain (NC) are noted (two-tailed *t*-test; * $p < 0.05$, ** $p < 0.01$). ns—not significant.

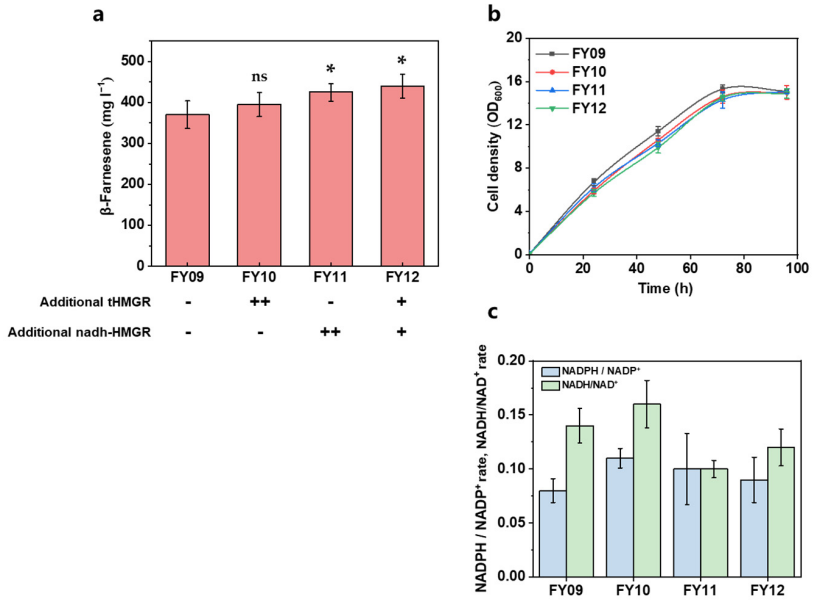

Figure 4. Further overexpression of rate-limiting enzyme HMG-CoA reductase. (**a**) β-Farnesene production by expression of additional copies of NADH or NADPH-dependent HMG-CoA reduction and (**b**) cell density. (**c**) Intracellular NADPH/NADP+ and NADH/NAD+ ratios. β-Farnesene was detected at 96 h of fermentation. Each black plus sign represents a copy. Data are represented as mean ± standard deviation (n = 3). Statistically significant differences between each engineered β-farnesene production strain and control strain (NC) are noted (two-tailed *t*-test; ns—not significant; * $p < 0.05$).

To prove our conjecture, the intracellular NADPH/NADP$^+$ and NADH/NAD$^+$ ratios were determined for the cell samples at 72 h (Figure 4c). No significant changes in intracellular NADPH/NADP$^+$ ratios among the four experimental strains were observed, which may be due to the high endogenous NADPH synthesis flux in *Y. lipolytica*, in which glucose can produce sufficient NADPH for β-farnesene production via the pentose phosphate pathway [48,49]. On the other hand, three to four copies of *tHMGR* may be sufficient to meet the demand of the MVA pathway for intracellular NADPH. In contrast, the intracellular NADH/NAD$^+$ ratio of the *nadh-HMGR*-enhanced strain decreased substantially, which may, to some extent, reflect that the intracellular NADH pool of *Y. lipolytica* is depleted by the MVA pathway and further enhances β-farnesene production. We considered that the modification strategies based on the current strain effectively pulled the carbon flow into the β-farnesene synthesis pathway.

Iterative intensification of the MVA pathway may saturate the conversion capacity of a single copy of β-farnesene synthase in strain FY12. Thus, an additional one or two copies of *aaBFS* were integrated into strain FY12, resulting in strains FY13 and FY14, respectively. Further expression of both single-copy and double-copy aaBFS strains showed only a small elevation of β-farnesene titer. Specifically, the β-farnesene titer of strains FY13 (473 ± 19.5 mg L^{-1}) and FY14 (480 ± 27.8 mg L^{-1}) was 8.7% and 10.3% higher, respectively, than that of control strain FY12 (Figure 5a). The results show that the additional β-farnesene synthase consumed the remaining MVA pathway intermediates, and the limited β-farnesene titer enhancement reflected the high FPP conversion efficiency of *aaBFS*.

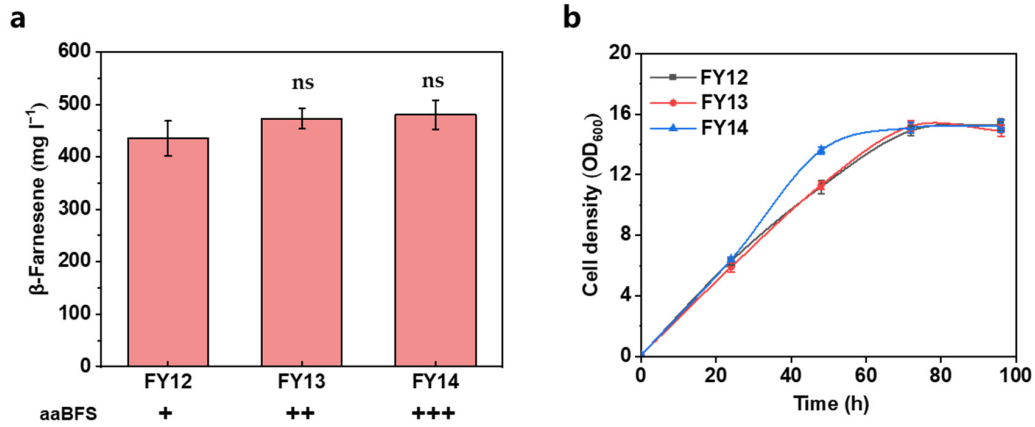

Figure 5. (**a**) Effect of increasing copy number of *aaBFS* on β-farnesene titer and (**b**) cell density. Each black plus sign represents a copy. β-Farnesene was detected at 96 h of fermentation. Data are represented as mean ± standard deviation (n = 3). Statistically significant differences between each engineered β-farnesene production strain and control strain (NC) are noted (two-tailed *t*-test; ns—not significant).

Overall, the orthogonal iterative enhancement of MVA pathway genes, HMG-CoA reductase, and β-farnesene synthase significantly enhanced the metabolic flux and production ability of β-farnesene in engineered *Y. lipolytica*. According to our assumption, the limiting factor in the enhancement of synthesis capacity of β-farnesene in the current strain was the supply of cytosolic acetyl-CoA. Increasing the availability of the intracellular precursor acetyl-CoA pool has been shown to be an effective strategy for enhancing terpenoid production [50]. In *Y. lipolytica*, mitochondrial citrate is transported into the cytoplasm, where it can be cleaved by ATP citrate lyase (ACL) to acetyl-CoA and oxaloacetate, with concomitant hydrolysis of 1 ATP molecule for ADP [51]. Overexpression of and screening for ACL helps to enhance the cytoplasmic acetyl-CoA supply. It has been reported that *Saccharomyces cerevisiae* can be engineered to employ the carnitine shuttle for export of acetyl moieties from the mitochondria, thereby supplementing cytoplasmic acetyl-CoA [52]. In addition, one study combined acetaldehyde dehydrogenase (ADA) with xylulose-5-phosphate phosphoketolase (xPK) and phosphotransacetylase (PTA) to substi-

tute the pyruvate dehydrogenase bypass (PDH-bypass) in *Saccharomyces cerevisiae* [16]. We consider that a similar strategy could be applied to further enhance β-farnesene production in our current strain.

3.3. Establishing Lignocellulosic Hydrolysate Utilization Strategy in Fermentation Media

Lignocellulosic biomass produced from agricultural waste is considered to be an alternative to traditional fermentation feedstocks. Glucose and xylose are the two main hydrolysis products of lignocellulose. The lignocellulose hydrolysate (LH) media used in this study contained 40.3 ± 0.4 g L^{-1} of glucose and 14.7 ± 0.3 g L^{-1} of xylose (Table 2). We investigated the growth and β-farnesene synthesis capacity of strain FY14 in LH media. To explore the effect of different lignocellulosic hydrolysate concentrations, we used 100% LH media and 75 and 50% diluted LH media for fermentation. The overall trends in 100 and 75% LH media showed that there was no significant effect of lignocellulose hydrolysate concentration on cell growth. Compared to the other two groups, strain FY14 appeared to have significantly lower biomass in 50% LH media, because glucose was depleted within 72 h, and the initial 20 g L^{-1} of glucose in 50% LH media was not sufficient to support subsequent cell growth (Figure 6b–d). Similar results were found in β-farnesene production: the β-farnesene titer in 100 and 75% LH media was 379 ± 29.2 and 374 ± 25.2 mg L^{-1}, respectively, while it was 242 ± 33.2 mg L^{-1} in 50% LH media (Figure 6a).

Table 2. Concentrations of fermentable fractions in lignocellulose hydrolysate.

Sample	Glucose (g L^{-1})	Xylose (g L^{-1})	Acetic Acid (g L^{-1})	Furfural (g L^{-1})	5-Hydroxymethylfurfurals (g L^{-1})	Soluble Lignin (g L^{-1})
Hydrolysate	40.3 ± 0.4	14.7 ± 0.3	1.4 ± 0.04	1.30 ± 0.07	0.70 ± 0.02	0.31 ± 0.02
Concentrated hydrolysate	107.4 ± 0.6	39.17 ± 0.5	3.73 ± 0.06	3.46 ± 0.09	1.86 ± 0.03	0.83 ± 0.01
Detoxified hydrolysate	102.3 ± 0.6	37.6 ± 0.3	3.62 ± 0.05	0	0	0.12 ± 0.01

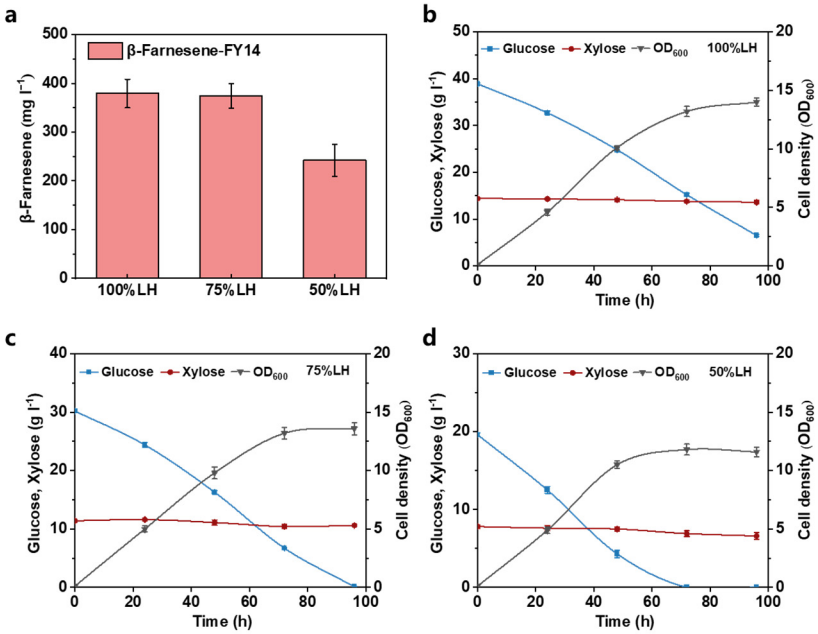

Figure 6. Fermentation results of strain FY14. (**a**) Titer of β-farnesene in 100%, 75%, and 50% LH media. (**b**–**d**) Cell density, glucose, and xylose consumption curves for 100%, 75%, and 50% LH media, respectively. β-Farnesene was detected at 96 h of fermentation. Data are represented as mean ± standard deviation (n = 3).

Due to the influence of cryptic genetic circuits that control the expression of key enzymes in metabolic pathways, *Y. lipolytica* cannot grow on xylose as a single carbon source, although a natural xylose pathway exists [53]. Although glucose is depleted in the late stages of fermentation, xylose in the LH media was basically unused during the fermentation process (Figure 6b–d). The small amount of acetic acid in the media was quickly consumed due to the endogenous acetyl-CoA synthase in *Y. lipolytica* (data not shown) [54]. In addition, compared with our previous experiments, the β-farnesene production and cell density of strain FY14 were lower in LH media than in YNBG media (Figure 5a,b and Figure 6a–d). This is because several types of inhibitors, such as furan derivatives, phenolic compounds, and weak acids, are produced during most lignocellulosic pretreatments [55]. Furfural, 5-hydroxymethylfurfurals, and soluble lignin were detected in the hydrolysate used in this study (Table 2). Although it is generally accepted that *Y. lipolytica* is tolerant to some organic acids [18], the accumulation of inhibitors in the lignocellulose hydrolysate can still have a significant impact on cell growth and production. To address the unavailability of xylose during fermentation, the engineered strain can be improved by introducing a heterologous xylose metabolic pathway in conjunction with directed laboratory evolution [56]. In addition, reusing the remaining xylose in the fermentation broth with metabolizable xylose strains is an economical route for a modified fermentation process. Similarly, strain tolerance tests allow the screening of *Y. lipolytica* mutants with excellent resistance to high concentrations of lignocellulose hydrolysate under fermentation conditions.

Metal ions and trace elements are important for the physiological and biochemical reactions of cells and are important factors affecting microbial growth and metabolite biosynthesis [57]. Similar to most terpene synthases, β-farnesene synthase activity is also influenced by the type and concentration of metal ions [58]. Therefore, we investigated the effect of adding YNB, Mg^{2+}, Mn^{2+}, and Fe^{2+} on the fermentation results. YNB was added at a concentration of 1.5 g/L, metal ions were added at a concentration of 5 mM, and all metal ions were added to the 100% LH media as sulfate.

The addition of YNB had no significant effect on the production of β-farnesene, which we speculated was due to the presence of some trace elements necessary for cell growth in the lignocellulose hydrolysate. Among the three metal ions, only the addition of Mg^{2+} slightly improved the synthesis of β-farnesene (435 ± 29.9 mg L^{-1}) (Figure 7). As consistent with previous findings, Mg^{2+} binding is particularly important for the catalytic function of β-farnesene synthase [58]. The addition of Fe^{2+} slightly reduced β-farnesene production, which may be due to the inhibition of certain intracellular metabolic reactions by the addition of excess Fe^{2+}. Based on the results of this part, we used 100% LH media supplemented with 5 mM magnesium sulfate in subsequent experiments.

3.4. Upscaling Fermentation in 2 L Fermenter

In order to test the performance of the engineered strains in scaled-up fermentation, we carried out fed-batch fermentation in a 2 L fermenter.

During the fermentation process, the highest cell density reached was 112 ± 3.5 (OD_{600}), β-farnesene titer reached 7.38 ± 0.24 g L^{-1} at 144 h, and the yield of β-farnesene was 0.075 g g^{-1} glucose (Figure 8). During fed-batch fermentation, the xylose in the lignocellulose hydrolysate was still not efficiently used, and the xylose in the fermentation broth increased in a stepwise manner with the replenishment of the feed solution. There was a small amount of spilled citrate from the TCA cycle, but the concentration was less than 5.5 g L^{-1}. These results indicate that the multi-gene iterative enhancement strategy in this study was successful and that the final strain FY14 had good β-farnesene production performance in lignocellulose hydrolysate media. The 7.38 ± 0.24 g L^{-1} titer represents the highest β-farnesene production from lignocellulose hydrolysate reported thus far, and has the potential to be enhanced by further fermentation optimization.

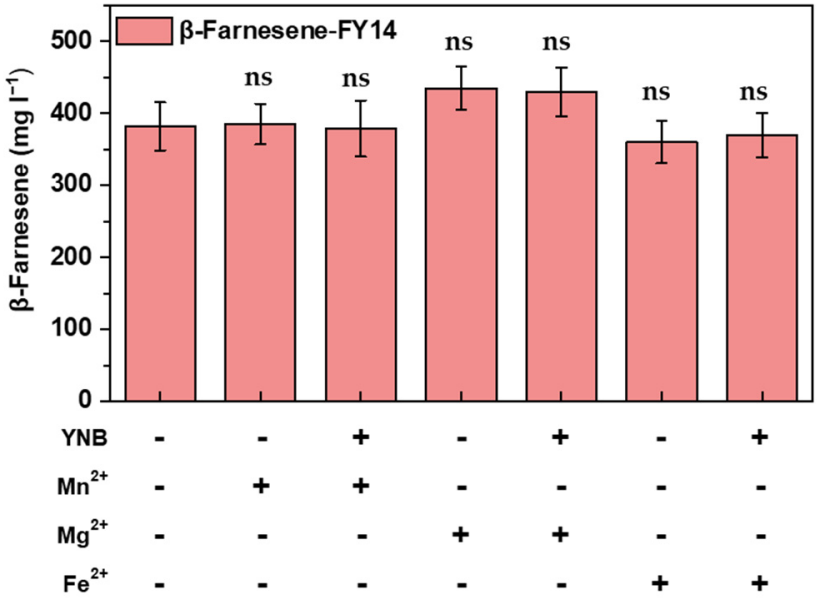

Figure 7. Effect of adding YNB and metal ions on β-farnesene production. β-Farnesene was detected at 96 h of fermentation. Data are represented as mean ± standard deviation (n = 3). Statistically significant differences between each engineered β-farnesene production strain and control strain (NC) are noted (two-tailed *t*-test; ns—not significant).

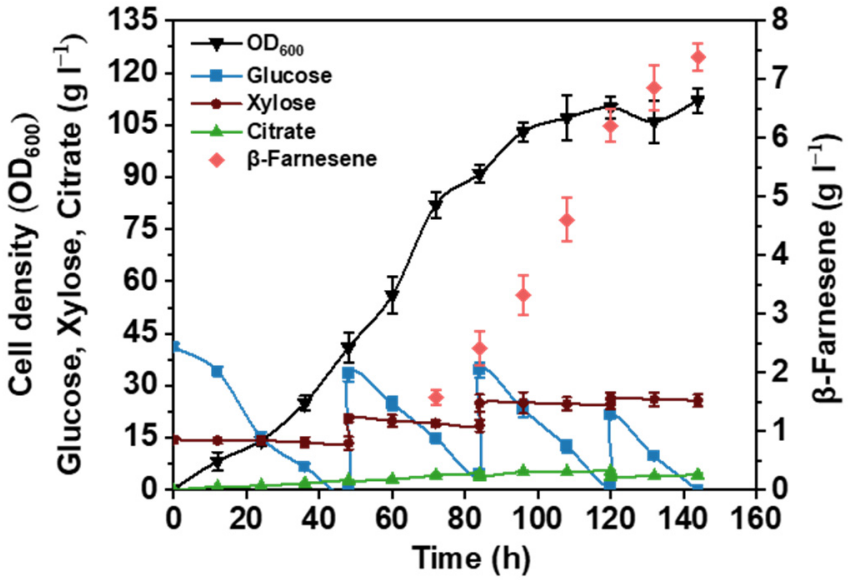

Figure 8. β-Farnesene titer, glucose and xylose consumption, citric acid accumulation, and cell density of strain FY14 in fed-batch fermentation. Data are represented as mean ± standard deviation (n = 3).

4. Conclusions

In this study, *Y. lipolytica* engineered for producing β-farnesene from lignocellulose hydrolysate was designed and constructed. To this end, the MVA pathway, HMG-CoA reductase, and optimal β-farnesene synthase were iteratively orthogonally enhanced, which significantly increased the β-farnesene production of the recombinant strains, and heterologous NADH-dependent HMGR was expressed to enhance the utilization of intracellular NADH. Media containing 100% lignocellulose hydrolysate and 5 mM magnesium sulfate was used for β-farnesene production. The titer and yield of β-farnesene finally reached 7.38 ± 0.24 g L^{-1} and 0.075 g g^{-1} glucose, respectively, using lignocellulose hydrolysate

media. To our knowledge, this is the first study on the biosynthesis of β-farnesene from lignocellulose hydrolysate in *Y. lipolytica*. Our results suggest that *Y. lipolytica* has the potential to become a platform for the biosynthesis of high-value-added products from low-cost agricultural waste.

Supplementary Materials: The following supporting information can be downloaded at https://www.mdpi.com/article/10.3390/fermentation8100532/s1. Table S1: Plasmids used in this work; Table S2: Primers used in this work; Table S3: The exogenous DNA used in this study; Figure S1: Schematic representation of gene chromosome integration in this study and schematic representation of pRSF vector backbone.

Author Contributions: Conceptualization, H.B., M.W. and Y.F.; data curation, H.B.; formal analysis, C.X.; methodology, H.B., C.S., P.F. and C.Z.; supervision, M.W. and T.T.; validation, H.B. and C.X.; writing—original draft, H.B., M.W. and Y.F. All authors have read and agreed to the published version of the manuscript.

Funding: The research was supported by National Key Research and Development Program of China (No. 2021YFC2103703).

Institutional Review Board Statement: Not applicable.

Informed Consent Statement: Not applicable.

Data Availability Statement: Not applicable.

Conflicts of Interest: The authors declare no conflict of interest.

References

1. Huelin, F.E.; Murray, K.E. α-Farnesene in the natural coating of apples. *Nature* **1966**, *210*, 1260–1261. [CrossRef] [PubMed]
2. Su, S.; Liu, X.; Pan, G.; Hou, X.; Zhang, H.; Yuan, Y. In vitro characterization of a (E)-beta-farnesene synthase from Matricaria recutita L. and its up-regulation by methyl jasmonate. *Gene* **2015**, *571*, 58–64. [CrossRef]
3. Yu, X.; Jones, H.D.; Ma, Y.; Wang, G.; Xu, Z.; Zhang, B.; Zhang, Y.; Ren, G.; Pickett, J.A.; Xia, L. (E)-beta-Farnesene synthase genes affect aphid (Myzus persicae) infestation in tobacco (Nicotiana tabacum). *Funct. Integr. Genom.* **2012**, *12*, 207–213. [CrossRef]
4. Liu, J.; Zhao, X.; Zhan, Y.; Wang, K.; Francis, F.; Liu, Y. New slow release mixture of (E)-β-farnesene with methyl salicylate to enhance aphid biocontrol efficacy in wheat ecosystem. *Pest Manag. Sci.* **2021**, *77*, 3341–3348. [CrossRef]
5. You, S.; Yin, Q.; Zhang, J.; Zhang, C.; Qi, W.; Gao, L.; Tao, Z.; Su, R.; He, Z. Utilization of biodiesel by-product as substrate for high-production of β-farnesene via relatively balanced mevalonate pathway in Escherichia coli. *Bioresour. Technol.* **2017**, *243*, 228–236. [CrossRef]
6. George, K.W.; Alonso-Gutierrez, J.; Keasling, J.D.; Lee, T.S. Isoprenoid Drugs, Biofuels, and Chemicals—Artemisinin, Farnesene, and Beyond. In *Biotechnology of Isoprenoids*; Schrader, J., Bohlmann, J., Eds.; Springer International Publishing: Cham, Switzerland, 2015; pp. 355–389.
7. Akutagawa, S.; Taketomi, T.; Kumobayashi, H.; Takayama, K.; Someya, T.; Otsuka, S. Metal-Assisted Terpenoid Synthesis. V. The Catalytic Trimerization of Isoprene to trans-β-Farnesene and Its Synthetic Applications for Terpenoids. *Bull. Chem. Soc. Jpn.* **1978**, *51*, 1158–1162. [CrossRef]
8. Arkoudis, E.; Stratakis, M. Synthesis of Cordiaquinones B, C, J, and K on the Basis of a Bioinspired Approach and the Revision of the Relative Stereochemistry of Cordiaquinone C. *J. Org. Chem.* **2008**, *73*, 4484–4490. [CrossRef] [PubMed]
9. Ford, T.J.; Silver, P.A. Synthetic biology expands chemical control of microorganisms. *Curr. Opin. Chem. Biol.* **2015**, *28*, 20–28. [CrossRef] [PubMed]
10. Woolston, B.M.; Edgar, S.; Stephanopoulos, G. Metabolic Engineering, Past and Future. *Annu. Rev. Chem. Biomol. Eng.* **2013**, *4*, 259–288. [CrossRef]
11. Yao, P.; You, S.; Qi, W.; Su, R.; He, Z. Investigation of fermentation conditions of biodiesel by-products for high production of β-farnesene by an engineered Escherichia coli. *Environ. Sci. Pollut. R* **2020**, *27*, 22758–22769. [CrossRef] [PubMed]
12. You, S.; Chang, H.; Zhang, C.; Gao, L.; Qi, W.; Tao, Z.; Su, R.; He, Z. Recycling strategy and repression elimination for lignocellulosic-based farnesene production with an engineered Escherichia coli. *J. Agric. Food Chem.* **2019**, *67*, 9858–9867. [CrossRef] [PubMed]
13. Tippmann, S.; Anfelt, J.; David, F.; Rand, J.M.; Siewers, V.; Uhlén, M.; Nielsen, J.; Hudson, E.P. Affibody scaffolds improve sesquiterpene production in Saccharomyces cerevisiae. *ACS Synth. Biol.* **2017**, *6*, 19–28. [CrossRef] [PubMed]
14. Tippmann, S.; Ferreira, R.; Siewers, V.; Nielsen, J.; Chen, Y. Effects of acetoacetyl-CoA synthase expression on production of farnesene in Saccharomyces cerevisiae. *J. Ind. Microbiol. Biotechnol.* **2017**, *44*, 911–922. [CrossRef] [PubMed]
15. Tippmann, S.; Scalcinati, G.; Siewers, V.; Nielsen, J. Production of farnesene and santalene by Saccharomyces cerevisiae using fed-batch cultivations with RQ-controlled feed. *Biotechnol. Bioeng.* **2016**, *113*, 72–81. [CrossRef]

16. Meadows, A.L.; Hawkins, K.M.; Tsegaye, Y.; Antipov, E.; Kim, Y.; Raetz, L.; Dahl, R.H.; Tai, A.; Mahatdejkul-Meadows, T.; Xu, L.; et al. Rewriting yeast central carbon metabolism for industrial isoprenoid production. *Nature* **2016**, *537*, 694–697. [CrossRef]
17. Shi, T.; Li, Y.; Zhu, L.; Tong, Y.; Yang, J.; Fang, Y.; Wang, M.; Zhang, J.; Jiang, Y.; Yang, S. Engineering the oleaginous yeast Yarrowia lipolytica for β-farnesene overproduction. *Biotechnol. J.* **2021**, *16*, 2100097. [CrossRef]
18. Abdel-Mawgoud, A.M.; Markham, K.A.; Palmer, C.M.; Liu, N.; Stephanopoulos, G.; Alper, H.S. Metabolic engineering in the host Yarrowia lipolytica. *Metab. Eng.* **2018**, *50*, 192–208. [CrossRef]
19. Liu, H.-H.; Ji, X.-J.; Huang, H. Biotechnological applications of Yarrowia lipolytica, Past, present and future. *Biotechnol. Adv.* **2015**, *33*, 1522–1546. [CrossRef]
20. Gao, S.; Tong, Y.; Zhu, L.; Ge, M.; Zhang, Y.; Chen, D.; Jiang, Y.; Yang, S. Iterative integration of multiple-copy pathway genes in Yarrowia lipolytica for heterologous β-carotene production. *Metab. Eng.* **2017**, *41*, 192–201. [CrossRef]
21. Tang, W.-Y.; Wang, D.-P.; Tian, Y.; Fan, X.; Wang, C.; Lu, X.-Y.; Li, P.-W.; Ji, X.-J.; Liu, H.-H. Metabolic engineering of Yarrowia lipolytica for improving squalene production. *Bioresour. Technol.* **2021**, *323*, 124652. [CrossRef]
22. Shaikh, K.M.; Odaneth, A.A. Metabolic engineering of Yarrowia lipolytica for the production of isoprene. *Biotechnol. Prog.* **2021**, *37*, e3201. [CrossRef] [PubMed]
23. Wang, C.; Liwei, M.; Park, J.-B.; Jeong, S.-H.; Wei, G.; Wang, Y.; Kim, S.-W. Microbial Platform for Terpenoid Production, Escherichia coli and Yeast. *Front. Microbiol.* **2018**, *9*, 2460. [CrossRef] [PubMed]
24. Qing, Q.; Guo, Q.; Wang, P.; Qian, H.; Gao, X.; Zhang, Y. Kinetics study of levulinic acid production from corncobs by tin tetrachloride as catalyst. *Bioresour. Technol.* **2018**, *260*, 150–156. [CrossRef]
25. Wang, Y.; Li, S.; Ma, L.; Dong, S.; Liu, L. Corn stalk as starting material to prepare a novel adsorbent via SET-LRP and its adsorption performance for Pb(II) and Cu(II). *R Soc. Open Sci.* **2020**, *7*, 191811. [CrossRef] [PubMed]
26. Wu, M.; Gao, F.; Yin, D.M.; Luo, Q.; Fu, Z.Q.; Zhou, Y.G. Processing of Superfine Grinding Corn Straw Fiber-Reinforced Starch Film and the Enhancement on Its Mechanical Properties. *Polymers* **2018**, *10*, 855. [CrossRef]
27. Xu, W.; Fu, S.; Yang, Z.; Lu, J.; Guo, R. Improved methane production from corn straw by microaerobic pretreatment with a pure bacteria system. *Bioresour. Technol.* **2018**, *259*, 18–23. [CrossRef]
28. Yang, X.; Cheng, L.; Yin, C.; Lebailly, P.; Azadi, H. Urban residents' willingness to pay for corn straw burning ban in Henan, China, Application of payment card. *J. Clean. Prod.* **2018**, *193*, 471–478. [CrossRef]
29. Jia, F.; Liu, H.-J.; Zhang, G.-G. Preparation of carboxymethyl cellulose from corncob. *Procedia Environ. Sci.* **2016**, *31*, 98–102. [CrossRef]
30. Fujiwara, R.; Noda, S.; Tanaka, T.; Kondo, A. Metabolic engineering of Escherichia coli for shikimate pathway derivative production from glucose-xylose co-substrate. *Nat. Commun.* **2020**, *11*, 279. [CrossRef]
31. Shen, L.; Kohlhaas, M.; Enoki, J.; Meier, R.; Schönenberger, B.; Wohlgemuth, R.; Kourist, R.; Niemeyer, F.; van Niekerk, D.; Bräsen, C.; et al. A combined experimental and modelling approach for the Weimberg pathway optimization. *Nat. Commun.* **2020**, *11*, 1098. [CrossRef]
32. Zhao, J.; Xia, L. Bioconversion of corn stover hydrolysate to ethanol by a recombinant yeast strain. *Fuel Process. Technol.* **2010**, *91*, 1807–1811. [CrossRef]
33. Qureshi, N.; Cotta, M.A.; Saha, B.C. Bioconversion of barley straw and corn stover to butanol (a biofuel) in integrated fermentation and simultaneous product recovery bioreactors. *Food Bioprod. Process.* **2014**, *92*, 298–308. [CrossRef]
34. Rodrigues, R.C.; Kenealy, W.R.; Jeffries, T.W. Xylitol production from DEO hydrolysate of corn stover by Pichia stipitis YS-30. *J. Ind. Microbiol. Biotechnol.* **2011**, *38*, 1649–1655. [CrossRef]
35. Cao, G.; Ren, N.; Wang, A.; Lee, D.-J.; Guo, W.; Liu, B.; Feng, Y.; Zhao, Q. Acid hydrolysis of corn stover for biohydrogen production using Thermoanaerobacterium thermosaccharolyticum W16. *Int. J. Hydrogen Energy* **2009**, *34*, 7182–7188. [CrossRef]
36. Gibson, D.G.; Young, L.; Chuang, R.Y.; Venter, J.C.; Hutchison, C.A.; Smith, H.O. Enzymatic assembly of DNA molecules up to several hundred kilobases. *Nat. Methods* **2009**, *6*, 343–345. [CrossRef] [PubMed]
37. Holkenbrink, C.; Dam, M.I.; Kildegaard, K.R.; Beder, J.; Dahlin, J.; Doménech Belda, D.; Borodina, I. EasyCloneYALI, CRISPR/Cas9-based synthetic toolbox for engineering of the yeast Yarrowia lipolytica. *Biotechnol. J.* **2018**, *13*, 1700543. [CrossRef]
38. Lu, Y.; Wang, Y.; Xu, G.; Chu, J.; Zhuang, Y.; Zhang, S. Influence of High Solid Concentration on Enzymatic Hydrolysis and Fermentation of Steam-Exploded Corn Stover Biomass. *Appl. Biochem. Biotech.* **2010**, *160*, 360–369. [CrossRef] [PubMed]
39. Schwartz, C.; Frogue, K.; Ramesh, A.; Misa, J.; Wheeldon, I. CRISPRi repression of nonhomologous end-joining for enhanced genome engineering via homologous recombination in Yarrowia lipolytica. *Biotechnol. Bioeng.* **2017**, *114*, 2896–2906. [CrossRef]
40. Tai, M.; Stephanopoulos, G. Engineering the push and pull of lipid biosynthesis in oleaginous yeast Yarrowia lipolytica for biofuel production. *Metab. Eng.* **2013**, *15*, 1–9. [CrossRef]
41. Blazeck, J.; Liu, L.; Redden, H.; Alper, H. Tuning gene expression in Yarrowia lipolytica by a hybrid promoter approach. *Appl. Environ. Microbiol.* **2011**, *77*, 7905–7914. [CrossRef]
42. Maruyama, T.; Ito, M.; Honda, G. Molecular Cloning, Functional Expression and Characterization of (E)-β-Farnesene Synthase from Citrus junos. *Biol. Pharm. Bull.* **2001**, *24*, 1171–1175. [CrossRef] [PubMed]
43. Yuan, J.; Ching, C.B. Mitochondrial acetyl-CoA utilization pathway for terpenoid productions. *Metab. Eng.* **2016**, *38*, 303–309. [CrossRef] [PubMed]
44. Xie, W.; Ye, L.; Lv, X.; Xu, H.; Yu, H. Sequential control of biosynthetic pathways for balanced utilization of metabolic intermediates in Saccharomyces cerevisiae. *Metab. Eng.* **2015**, *28*, 8–18. [CrossRef]

45. Chandran, S.S.; Kealey, J.T.; Reeves, C.D. Microbial production of isoprenoids. *Process Biochem.* **2011**, *46*, 1703–1710. [CrossRef]
46. Kwak, S.; Kim, S.R.; Xu, H.; Zhang, G.-C.; Lane, S.; Kim, H.; Jin, Y.-S. Enhanced isoprenoid production from xylose by engineered Saccharomyces cerevisiae. *Biotechnol. Bioeng.* **2017**, *114*, 2581–2591. [CrossRef] [PubMed]
47. Zuo, Y.; Xiao, F.; Gao, J.; Ye, C.; Jiang, L.; Dong, C.; Lian, J. Establishing Komagataella phaffii as a Cell Factory for Efficient Production of Sesquiterpenoid α-Santalene. *J. Agric. Food Chem.* **2022**, *70*, 8024–8031. [CrossRef] [PubMed]
48. Liu, N.; Qiao, K.; Stephanopoulos, G. (13)C Metabolic Flux Analysis of acetate conversion to lipids by Yarrowia lipolytica. *Metab. Eng.* **2016**, *38*, 86–97. [CrossRef] [PubMed]
49. Wasylenko, T.M.; Ahn, W.S.; Stephanopoulos, G. The oxidative pentose phosphate pathway is the primary source of NADPH for lipid overproduction from glucose in Yarrowia lipolytica. *Metab. Eng.* **2015**, *30*, 27–39. [CrossRef] [PubMed]
50. Zhang, Y.; Nielsen, J.; Liu, Z. Engineering yeast metabolism for production of terpenoids for use as perfume ingredients, pharmaceuticals and biofuels. *FEMS Yeast Res.* **2017**, *17*, fox080. [CrossRef] [PubMed]
51. Bellou, S.; Triantaphyllidou, I.-E.; Mizerakis, P.; Aggelis, G. High lipid accumulation in Yarrowia lipolytica cultivated under double limitation of nitrogen and magnesium. *J. Biotechnol.* **2016**, *234*, 116–126. [CrossRef]
52. van Rossum, H.M.; Kozak, B.U.; Niemeijer, M.S.; Dykstra, J.C.; Luttik, M.A.; Daran, J.M.G.; Van Maris, A.J.; Pronk, J.T. Requirements for Carnitine Shuttle-Mediated Translocation of Mitochondrial Acetyl Moieties to the Yeast Cytosol. *Mbio* **2016**, *7*, e00520-16. [CrossRef] [PubMed]
53. Rodriguez, G.M.; Hussain, M.S.; Gambill, L.; Gao, D.; Yaguchi, A.; Blenner, M. Engineering xylose utilization in Yarrowia lipolytica by understanding its cryptic xylose pathway. *Biotechnol. Biofuels* **2016**, *9*, 149. [CrossRef] [PubMed]
54. Park, Y.-K.; Bordes, F.; Letisse, F.; Nicaud, J.-M. Engineering precursor pools for increasing production of odd-chain fatty acids in Yarrowia lipolytica. *Metab. Eng. Commun.* **2021**, *12*, e00158. [CrossRef] [PubMed]
55. Yu, Y.; Liu, S.; Zhang, Y.; Lu, M.; Sha, Y.; Zhai, R.; Xu, Z.; Jin, M. A novel fermentation strategy for efficient xylose utilization and microbial lipid production in lignocellulosic hydrolysate. *Bioresour. Technol.* **2022**, *361*, 127624. [CrossRef] [PubMed]
56. Sun, T.; Yu, Y.; Wang, K.; Ledesma-Amaro, R.; Ji, X.-J. Engineering Yarrowia lipolytica to produce fuels and chemicals from xylose: A review. *Bioresour. Technol.* **2021**, *337*, 125484. [CrossRef] [PubMed]
57. Liu, Y.; Wang, Z.; Cui, Z.; Qi, Q.; Hou, J. α-Farnesene production from lipid by engineered Yarrowia lipolytica. *Bioresour. Bioprocess* **2021**, *8*, 78. [CrossRef]
58. Picaud, S.; Brodelius, M.; Brodelius, P. Expression, purification and characterization of recombinant (E)-β-farnesene synthase from Artemisia annua. *Phytochemistry* **2005**, *66*, 961–967. [CrossRef] [PubMed]